J Comp Physiol A (1993) 173:495–508

Journal of Comparative Physiology A Sensory, Neural, and Behavioral Physiology

Red and white muscle activity and kinematics of the escape response of the bluegill sunfish during swimming

B.C. Jayne[1], **G.V. Lauder**[2]

[1] Department of Biological Sciences, University of Cincinnati, Cincinnati, OH 45221-0006, USA
[2] Department of Ecology and Evolutionary Biology, University of California, Irvine, CA 92717, USA

Accepted: 13 April 1993

Summary. We quantified midline kinematics with synchronized electromyograms (emgs) from the red and white muscles on both sides of bluegill sunfish (*Lepomis macrochirus*) during escape behaviors which were elicited from fish both at a standstill and during steady speed swimming. Analyses of variance determined whether or not kinematic and emg variables differed significantly between muscle fiber types, among longitudinal positions, and between swimming versus standstill trials.

At a given longitudinal location, both the red and white muscle were usually activated synchronously during both stages of the escape behavior. Stage 1 emg onsets were synchronous; however, the mean durations of stage 1 emgs showed a significant increase posteriorly from about 11 to 15 ms. Stage 2 emgs had significant posterior propagation, but the duration of the stage 2 emgs was constant (17 ms). Posterior emgs from both stages occurred during lengthening of the contractile tissue (as indicated by lateral bending). Steady swimming activity was confined to red muscle bursts which were propagated posteriorly and had significant posterior decrease in duration from about 50% to 37% of a cycle. Fish performed escape responses during all phases of the steady swimming motor pattern. All kinematic events were propagated posteriorly. Furthermore, no distinct kinematic event corresponded to the time intervals of the stage 1 and 2 emgs. The rate of propagation of kinematic events was always slower than that of the muscle activity. The phase relationship between lateral displacement and lateral bending also changed along the length of the fish. Escape responses performed during swimming averaged smaller amplitudes of stage 2 posterior lateral displacement; however, most other kinematic and emg variables did not vary significantly between these two treatments.

Key words: Muscle – Locomotion – Fish – Electromyography – Kinematics

Abbreviations: A, angle of lateral flexion (bending) of midline at a single point in time; A1, A2, change in A from T_0 to T_1 and from T_1 to T_2; AMX, maximal lateral flexion concave towards the side of the stage 1 emg; AMXR, equals AMX minus A at T_0; AT1, AT2, lateral flexion at T_1 and T_2; DUR1, DUR2, durations of stage 1 and stage 2 emgs; emg, electromyogram ON2, onset time of stage 2 emg; RELDUR, relative duration of steady swimming emg; T_0, T_1, T_2, times of stage 1 emg onset, latest stage 1 emg offset and latest stage 2 emg offset standardized such that $T_0 = 0$; TAMX, TAMN, TYMX, times of maximal lateral flexion, no lateral flexion and maximum lateral displacement; Y1, Y2, amounts of lateral displacement from T_0 to T_1 and from T_1 to T_2; YMXR, relative amount of lateral displacement from T_0 to TYMX

Correspondence to: B.C. Jayne

Introduction

The escape response of fishes is one of the most rapid locomotor behaviors of vertebrates, and as such it is of great interest to such diverse areas as predator-prey ecology (Webb and Skadsen 1980), functional morphology (Webb 1978), muscle physiology (Wardle 1975; Rome and Sosnicki 1991) and neurophysiology (recent reviews: Eaton et al. 1991; Eaton and Hackett 1984). Electrophysiological studies have found that the latency between a sudden visual or vibrational stimulus and neuromuscular activity during the escape response may be less than 10 ms (Eaton et al. 1981). Extracellular recordings have found that the Mauthner cell is sufficient to cause the synchronous activation of the white musculature along the concave side of an initial C-shape formed by the fish (Zottoli 1977; Eaton et al. 1981), but alternative pathways can also yield similar behaviors which have all been collectively termed either fast-starts or escape responses (Eaton et al. 1982). The initial C-formation of the escape response is usually referred to as stage 1 (Weihs 1973), and Eaton et al. (1981) found that this stage had a higher degree of stereotypy than later events. Stage 1 electromyograms (emgs) are usually followed by high amplitude, contralateral emgs; however, with the exception of very recent work (Foreman and Eaton 1993), stage 2 neuromuscular activity is poorly understood compared

to that of stage 1. All previous electromyographic studies of the escape response have examined only events for fish that were initially at a standstill before they were startled. However, recent extracellular recordings from nerves in fictive preparations have begun to address how the escape response circuitry may interact with that involved in steady swimming (Fetcho 1992).

Early kinematic analyses of escape responses have shown that the movements associated with stage 1 may take less than 30 ms and are faster than any other locomotor behavior of fishes (Eaton et al. 1977; Webb 1978). To better understand how fish evade predators and respond to varying orientation of stimulus, additional analyses of the escape behavior have used diverse methods to determine the maximal velocities and trajectories as well as other indicators of the performance of the escape (Eaton et al. 1988; Eaton and Emberley 1991; Harper and Blake 1990; Covell et al. 1991). Several kinematic studies of steady undulatory locomotion of fishes have demonstrated that the waves of bending and displacement travel posteriorly along the length of the fish as it is propelled forward (Gray 1968; Webb 1975; Grillner and Kashin 1976; Williams et al. 1989). In contrast, the amplitude and timing of lateral bending during the escape behavior of fishes are poorly understood and these quantities have not been quantified simultaneously with electromyograms. However, during escapes, the fish's center of mass is known to remain stationary during the initial synchronous ipsilateral activation of muscle along the entire length of the fish (Eaton et al. 1988). Consequently, it is far from obvious from prior studies whether or not other kinematic and mechanical events occur in standing or travelling patterns during the different stages of the escape response. The extent of lateral bending is also of central importance to all undulatory locomotor behaviors including the escape response, because this kinematic variable is proportional to the magnitude of the strain undergone by the axial musculature (Rome and Sosnicki 1991; Johnston 1991; Van Leeuwen et al. 1990).

The purpose of this study was to quantify the in vivo patterns of red and white muscle activity during both stages of the escape response. Midline kinematics were quantified primarily to clarify the patterns of bending during the escape response and also to be used as a measure of the performance of the escape response. Escape responses were elicited from fish during steady swimming and contrasted with those performed at standstill in order to determine whether or not the steady swimming motor pattern interferes with that of the escape response and possibly affects the kinematics. We were particularly interested in clarifying whether muscle activity and kinematic events occurred in standing or traveling waves along the length of the fish. Thus, as much as was practical, we attempted to determine muscle activity and kinematics for the entire length of the fish by studying events at several longitudinal locations.

Materials and methods

Experimental subjects and protocol. We obtained bluegill sunfish (*Lepomis macrochirus*) from small ponds in southern and central California. All animals were housed individually in 10–20 gal aquaria with a constant temperature (20±2°C) and a 12:12 light: dark cycle. Average time in captivity before experiments approximated 3 months. We implanted and videotaped a total of 6 individuals. Standard and total lengths and mass ranged from 14.8–15.2 cm, 17.5–18.2 cm and 97–188 g, respectively.

We threw an object (rubber coated size c flashlight battery) into the flow tank (working section 20 × 20 × 50 cm) to impact the surface of the water (20°C) to obtain a total of 12 escape responses from each individual with an average recovery period of 20 min between successive trials. This procedure succesfully evoked the escape behavior in 68 of 70 attempts with the 6 individuals. For the first 8 trials, we alternately elicited escape responses during steady swimming of the fish and then from the same individual at a standstill, whereas the last 4 trials for each individual were all during steady swimming. The speed of the fish during steady swimming was controlled by adjusting the flow of the tank to about 1.6 total fish lengths/s. Within the order of the trials that were either during swimming or at a standstill, we attempted to drop the stimulus alternately to the left and then to the right of the fish. We attempted to position the fish near the center of the cross-sectional area of the working section of the flow tank. Whenever a fish was less than 3 cm from any wall of the tank at any time during stages 1 or 2 of the escape behavior (on 3 occasions), the trial was discarded and another was added until we obtained the desired sample size. At the conclusion of an experiment each fish was killed with an overdose of anesthetic and preserved in order to confirm electrode placement and take x-rays and anatomical measurements.

Electromyography. Anesthesia of fish was induced with a 0.06% buffered solution of tricaine methane sulfonate (MS222) prior to implanting electrodes. During the implantation, which lasted less than 2 h, anesthesia was maintained with a 0.03% solution of MS222, and a peristaltic pump circulated water over the gills of the fish at 10–15 min intervals. We made electrodes by stripping about 0.6 mm of insulation off the ends of stainless steel wire (0.051 mm diameter) about 2 m long. Greater details of electrode construction can be found in Jayne (1988). We implanted these bipolar electrodes into the fish percutaneously using 26 gauge sub-q (Becton-Dickinson) hypodermic needles. Electrodes were inserted into the left and right red axial muscle at each of 4 standardized longitudinal locations spaced approximately 5 vertebrae apart (Fig. 1). To record white muscle activity, we inserted additional electrodes dorsal and medial to the first and third red electrode sites. One additional electrode was placed in white muscle at varying locations (Fig. 1), but we did not analyze results from this site. The wires from all 13 electrodes were glued together into a single cable which was tied to one of the spines of the dorsal fin (Fig. 1). To minimize the effects of the fin on the cable and vice versa, we cut the fin membrane attached to this spine and trimmed fin spines anterior to this site. We left the most posterior fin spine intact and attached to the anterior portion of the soft dorsal fin. We chose our method of cable attachment because prior videotapes of bluegill swimming showed that the spiny portion of the dorsal fin was not normally involved in steady swimming, and we wanted to minimize disturbance to the functionally more significant (soft) part of the dorsal fin. Fish were allowed to recover for about 3 h before starting the experiments.

Electromyograms (emgs) were amplified 20,000 × using Grass model P511 K pre-amplifiers with high and low band pass filter settings of 100 Hz and 3 kHz and a 60 Hz notch filter. The emgs were recorded with a TEAC XR-5000 FM data recorder using a tape speed of 9.5 cm/s. We played back the emgs at one-eighth recording speed into a Keithley analog to digital converter which sampled data at 1 kHz allowing an effective sampling rate of 8 kHz for the digital emgs. Because the rapid movement of the escape behavior causes considerable low frequency artifacts, we filtered the digital emgs using a finite impulse response filter that reduced the

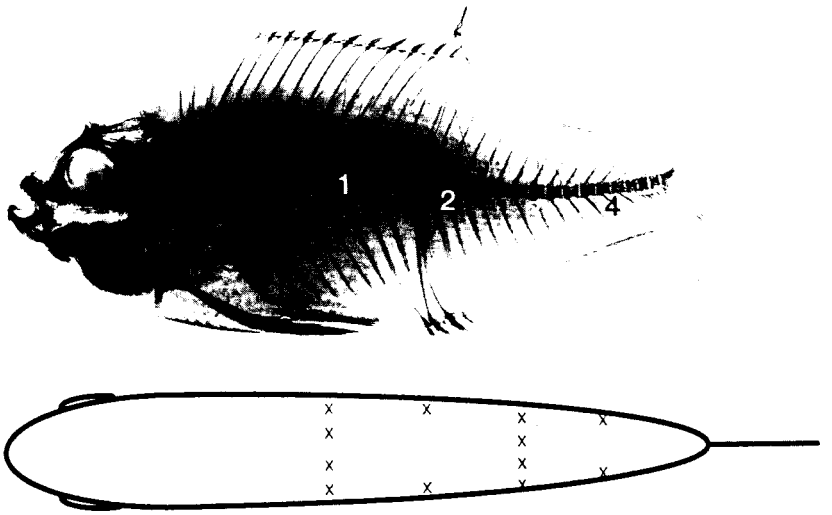

Fig. 1. Lateral x-ray of the longitudinal position of electrodes for recording muscle activity. The schematic dorsal view below the x-ray illustrates the overall pattern of electrode placement with *X*'s that are located most laterally indicating red muscle sites and those located more medially indicating white muscle sites

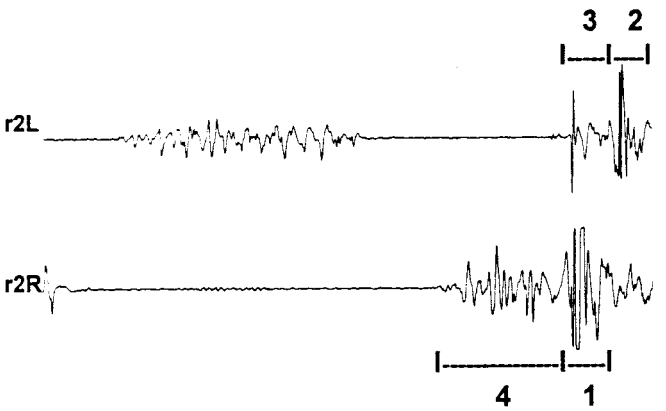

Fig. 2. Illustration of emg variables. Emgs are from the red muscle at electrode site 2 for an escape response (concave right) that occurred during swimming. *1* = duration of stage 1 emg (DUR1), *2* = duration of stage 2 (DUR2), *3* = time of stage 2 emg onset relative to the onset of stage 1 emg (ON1), and *4* = lag from onset of swimming emg ipsilateral to the onset of stage 1 emg (used to calculate phase)

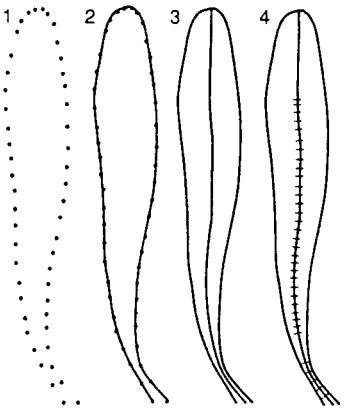

Fig. 3. Schematic diagram of computer method for reconstructing the midline of fish during swimming and c-starts. For each frame: *1*, the outline of the fish was digitized; *2*, the outline of the fish was reconstructed; *3*, the midline was generated using the x and y coordinates of the points comprising the reconstructed outline; and *4*, the midline was partitioned into anatomical lengths determined from x-rays

portion of the signal below 100 Hz to less than 10% of its original amplitude.

We quantified the time (±1ms) of various events (Fig. 2, Tables 1 and 2) using the filtered digital emgs and a custom computer program. Elapsed times were standardized so that zero equaled the onset of the stage 1 emg. We measured the duration of the stage 1 emg (DUR1) and the time of onset (ON2) and duration of the stage 2 emg (DUR2). Only the red muscle was used during the steady swimming prior to a C-start, and this pattern of activity consisted of bursts that regularly alternated between the right and left sides. We defined the duration of the period of the steady swimming emgs as the time between successive onsets, and we quantified the duration of steady swimming red emgs (RELDUR) as the percentage of the period for which there was activity. We calculated when the onset of the stage 1 emg occurred with respect to the phase of the steady swimming emg by dividing the lag between the onset of the last steady swimming emg by the duration of the last complete period prior to the C-start and multiplying the result by 360°.

Kinematics. We videotaped all trials with an NAC HSV-400 high-speed video system operating at 400 images/s. We obtained a ventral view of the fish via a front surface mirror mounted below the transparent bottom of the working section of the flow tank. Between 30 to 40 individual video images (spaced at 2.5 ms intervals) were digitized per trial, beginning about 10 ms prior to the onset of the stage 1 emg. Figure 3 schematically illustrates the method of obtaining motion data. We used a custom video digitizing program to measure the x and y coordinates of about 25 points that were manually placed along both the right and left sides of the fish. For each resulting digitized image, a different computer program used a cubic splice method to reconstruct the left and right outlines of the fish, and then the program calculated a midline between these two reconstructed outlines. Using anatomical measurements taken from x-rays of each fish, each midline was then partitioned into several line segments whose lengths corresponded to that of the skull, individual vertebrae, the tail bones and the caudal fin divided into portions one fifth of its resting length. Consequently, for each video image we obtained the x and y coordinates of each body segment as well as the angle of lateral bending between adjacent axial segments.

To reduce the kinematic data set (Tables 3 and 4) we primarily analyzed results from the following eight longitudinal locations:

snout, vertebrae 1, 5, vertebrae nearest the 4 electrode sites (approx. 10, 15, 20, 25), and a location along the caudal fin two-fifths its length posterior to the tail bones.

We have 3 groups of kinematic variables for time, lateral displacement and angle of lateral bending (Tables 3 and 4). These are distinguished by the following codes: T indicates time in ms, Y is the lateral displacement in mm and A is the angle of lateral bending in degrees. These codes are followed by MX or MN meaning maximum or minimum and R for relative. All times were standardized so that zero equaled onset of the stage 1 emg (T_0). T_1 and T_2 indicate the latest offset times of the stage 1 and stage 2 emgs, respectively.

We used the horizontal plane for our x-y coordinate plane (Fig. 9) with the x-axis parallel to: 1) the flow of the water, 2) the longest dimension of the working section of the flow tank and 3) the approximate longitudinal axis of the fish prior to the escape response. All lateral displacements (Y-coordinates) were standardized so that positive values indicate lateral displacement towards the side of the stage 1 emg, and the Y coordinates were adjusted so that Y of the first vertebrae at T_0 equaled zero. Angular measurements were standardized so that positive values indicate lateral bending that was concave towards the side of the stage 1 emg.

We measured the time of maximal lateral displacement towards the side opposite that of the stage 1 emg (TYMX). We also measured the time of maximal lateral bending (TAMX) concave towards the side of the stage 1 emg and the next time for which the region was straight (TAMN). We quantified the changes in lateral displacement ($Y1 = YT_1-YT_0$; $Y2 = YT_2-YT_1$) during stages 1 and 2 and determined the relative change in lateral displacement to attain a maximum (YMXR = maximum $Y-YT_0$). For lateral bending, we made homologous calculations for A1, A2 and AMXR. We also analyzed the amount of maximal bending concave towards the side of the stage 1 emg (AMX) and the lateral flexion (bending) at the ends of stage 1 and 2 emgs (AT1, AT2).

Statistical analysis. We quantified and analyzed emgs from the best five and kinematics from the best four preparations. We performed analyses of variance using a microcomputer statistical package (SPSS PC + 2). For all ANOVAs we considered individuals as random effects, whereas longitudinal location, swimming versus standstill, and red versus white muscle were all considered fixed effects. We followed the guidelines in Zar (1984) for performing appropriate F-test for the significance of each effect in mixed model ANOVAs. One should note that the F-value of a fixed main effect was calculated as the mean square (MS) of the fixed effect divided by the MS of the two way interaction term involving that fixed effect and the random effect. In contrast, the significance of the main random effect is tested by dividing MS of the random effect by the MS within cell error term.

Sample sizes for the ANOVAs of emg variables vary slightly because of the occasional inability to clearly detect the onset or offset of muscle activity as a result of either low amplitude or large motion artifacts (especially during stage 2). Analyses of variance of the red muscle emg variables were compared across all four electrode sites. Because of the difficulty of interpreting results of an ANOVA with more than three factors, we compared red to white emg variables separately for electrode sites 1 and 3.

For the analysis of the kinematic variables, data from all 16 C-starts from a standstill were used. One digitized sequence of a C-start during swimming produced unreliable midline results and was discarded leaving a total of 31 swimming trials used for statistical comparison of kinematics. Although descriptive statistics are included for the kinematic variables of locations at the snout and in the tail fin (sites 1 and 8, Table 4), ANOVAs testing for significant longitudinal variation were restricted to sites within the vertebral column. Furthermore, we felt that statistical tests of longitudinal variation in lateral bending were most meaningful for homologous anatomical structures (pairs of vertebrae). Consequently, in Table 3 there are 4 degrees of freedom associated with the site factor for A1, A2, AMXR, AMX, AT1 and AT2 which were analyzed for sites 3–7. Because an obvious peak value in lateral displacement could usually not be discerned at site 2 (Table 4) the ANOVAs of TYMX and YMXR were performed using only sites 3–7. All remaining kinematic variables were analyzed for all of the sites within the vertebral column (sites 2–7, Table 4). With the following exceptions, there were 16 standstill (st) and 31 swimming (sw) observations for all the kinematic variables in Table 4. For TYMX site 8 st; TAMN sites 2, 7,8 sw; TAMN sites 7,8, sample sizes were 15, 30, 28, 12, 12, and 7, respectively. These minor differences in sample sizes along with the variable number of sites analyzed account for the variable degrees of freedom given in Table 3.

Results

Electromyography

Figures 4–6 illustrate representative emgs for the each of the different experimental conditions. For escape re-

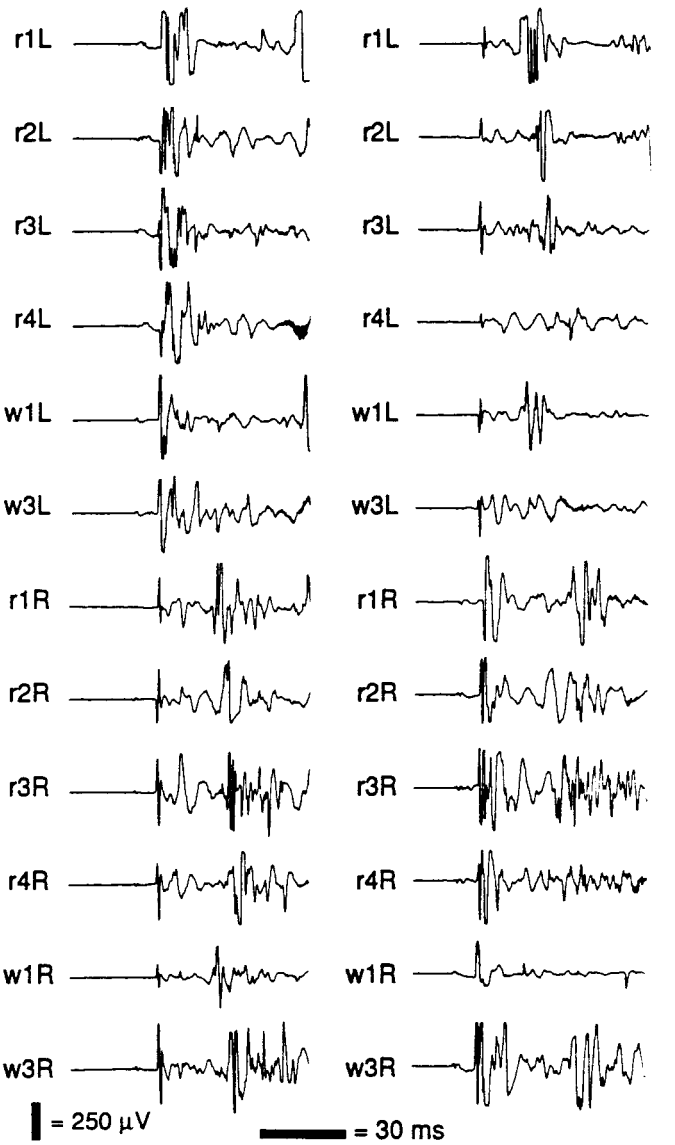

Fig. 4. Representative emgs from an escape response concave to the left (*left panel*) and concave to the right (*right panel*) from a single individual. Labeling of data channels is as follows: *r* and *w* indicate red and white muscle respectively, the *number* indicates the electrode position (see Fig. 1), and *L* and *R* indicate the left and right sides, respectively. All muscles in each panel were recorded simultaneously

Table 1. Summary of F-tests from ANOVAs performed separately on each electromyographic variable. For the three-way ANOVAs analyzing only data from in red muscle (top), factor A contrasts different longitudinal locations of electrode sites (Fig. 1), B contrasts swimming versus standstill c-starts, and C accounts for different individuals. Factor D (bottom) contrasts measurements from red versus white muscle at a single longitudinal position. Degrees of freedom for the mean squares are given below each term of the ANOVA model except those of the within cells error term which are given parenthetically after each emg EMG variable. See Materials and methods for more details of experimental design and sample sizes. ′, * and ** indicate $P<0.1$, 0.05 and 0.001, respectively

EMG Variable	ANOVA Effects						
	Site (A) 3	Swim (B) 1	Fish (C) 4	A*C 12	B*C 4	A*B 3	A*B*C 12
RELDUR (271)	26.9**		11.2**	2.5*			
DUR1 (200)	10.8*	0.9	4.9*	1.0	0.7	0.4	0.6
ON2 (163)	26.3**	4.1′	9.0**	0.9	2.7*	3.1′	0.8
DUR2 (163)	1.4	0.5	11.8**	1.6′	3.6*	0.7	0.6
	Fiber (D) 1	Swim (B) 1	Fish (C) 4	D*C 4	B*C 4	D*B 1	D*B*C 4
Electrode 1							
DUR1 (100)	2.7	0.1	2.2	0.5	0.4	3.7	0.2
ON2 (92)	3.5	0.02	2.9*	0.4	1.4	2.4	0.3
DUR2 (92)	1.2	10.0*	6.9**	1.1	0.9	0.4	1.5
Electrode 3							
DUR1 (99)	6.8′	2.0	3.0	0.5	0.7	0.2	0.7
ON2 (77)	1.9	3.1	5.5*	1.1	1.0	0.2	1.2
DUR2 (76)	19.8*	1.9	4.2*	0.4	0.5	0.02	2.0

Table 2. Mean values of emg variables pooled for swimming and standstill trials and across all 5 individuals that were used for the ANOVAs. After each mean the standard deviation and sample size are indicated parenthetically. For RELDUR, observations were included from both the right and left sides one period prior to the escape response. All values in ms except for RELDUR which is given in %

EMG Variable	Electrode Site			
	1	2	3	4
red				
RELDUR	50.9 (8.1, 60)	44.9 (4.9, 80)	37.6 (3.9, 72)	37.2 (6.1, 79)
DUR1	11.5 (2.9, 60)	13.4 (3.1, 60)	13.5 (2.7, 60)	14.7 (2.8, 60)
ON2	14.2 (2.7, 54)	17.1 (3.6, 54)	19.6 (4.0, 55)	18.4 (5.2, 40)
DUR2	17.4 (6.3, 55)	17.6 (5.1, 54)	15.6 (3.7, 54)	18.2 (5.2, 40)
white				
DUR1	12.3 (3.2, 60)		14.7 (4.0, 59)	
ON2	15.1 (3.0, 58)		18.9 (3.6, 42)	
DUR2	18.2 (5.0, 58)		18.2 (5.9, 42)	

sponses performed by fish at a standstill, the general pattern of muscle activity begins with simultaneous (within 1 ms) high amplitude emgs in the red and white muscle on the side of the fish's body that initially becomes laterally concave (Fig. 4). Excluding an initial brief potential, the contralateral side displays no regular pattern of activity during this first stage of the escape response. As illustrated in Fig. 4, escape responses performed towards opposite sides display the same pattern of emgs on the side that initially becomes concave during stage 1. Following the stage 1 emg, an additional high amplitude emg occurs in both the red and white muscle on the contralateral side. The bluegill were confined to a rather narrow flow tank out of the necessity to obtain steady swimming. However, the extreme similarity of our emgs with previously described emgs (reviewed in Eaton et al. 1991) and extracellular nerve recordings (Fetcho 1992) strongly suggests that we were indeed evoking similar escape behavior.

Emgs of escape responses during swimming were qualitatively similar to those from a standstill (Fig. 4 vs. 6). Similarly, the analysis of variance did not detect any significant differences in the duration of stage 1 emgs or the duration and onset time of the stage 2 emg (Table 1). The duration of the stage 2 white muscle emg at electrode site 1 was the only emg variable that differed between swimming (mean DUR2 = 16.9 ms) and standstill (mean DUR2 = 20.8 ms) trials. Thus, we conclude that the fish performed fundamentally the same escape behavior for these different initial conditions, and we pooled swimming and standstill trials to obtain the means of the emg variables shown in Table 2. There were also no highly significant differences in any of the emg variables when comparing red and white muscle (Table 1).

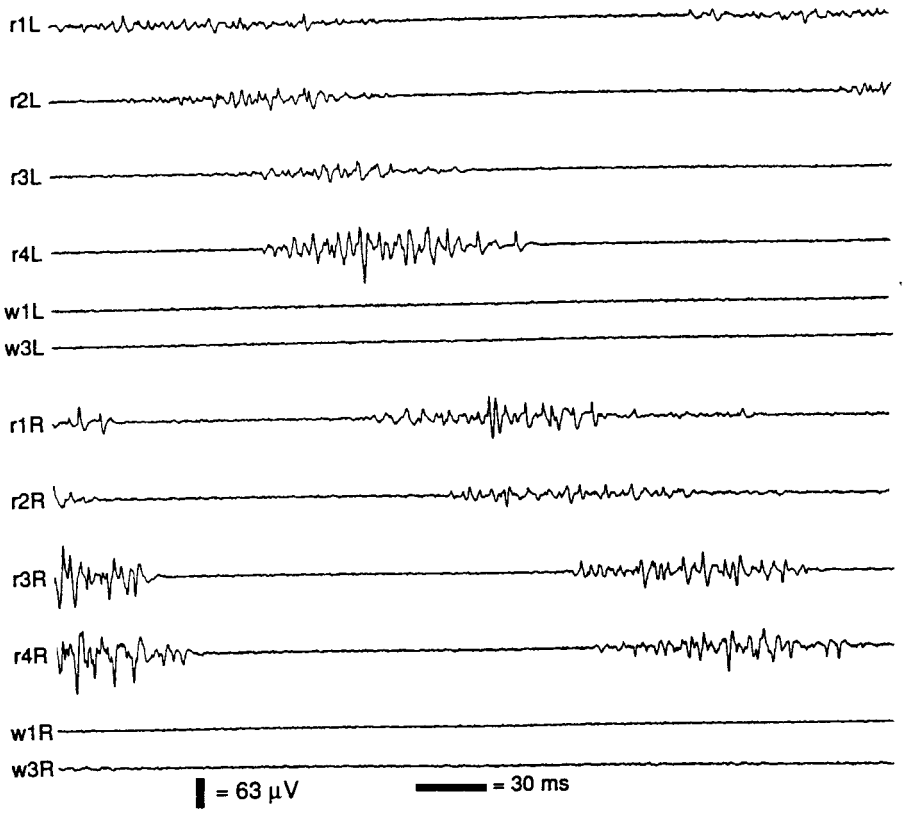

Fig. 5. Steady swimming emgs. Note that there is no white muscle activity, and the voltage scale is 1/4 that of Figs. 4 and 6. This fish (same as Fig. 4) was swimming steadily at about 1.6 lengths/s. All channels were recorded simultaneously

For the stage 1 red emgs, there was marginally significant longitudinal variation in duration which increased posteriorly from about 11 to 15 ms (electrodes 1 vs. 4, Table 2). The time of onset of the stage 2 emg increased significantly (Table 1) from about 14 to 20 ms. Therefore, in contrast to stage 1, the stage 2 emgs were propagated posteriorly. As shown in Table 2, the mean onset time for each of the four electrode sites always was greater than the duration of the stage 1 emg. Hence, at a given longitudinal location, 3 to 6 ms elapsed from the end of stage 1 until the onset of the stage 2 emg.

In contrast to the escape response, only the red muscle is used during the steady swimming of bluegill at 1.6 lengths/s (Fig. 5). The steady swimming emgs are: 1) propagated posteriorly , 2) mostly unilateral and 3) alternate between the right and left sides (Fig. 5). The duration of the steady swimming emgs had a significant decrease posteriorly (Table 1) from about 50% at electrode 1 to less than 40% of a cycle at electrode 4.

Figure 7 illustrates the phase of the steady swimming emgs at the time of onset of the stage 1 emg. At each site, we observed some stage 1 emgs beginning during ipsilateral (Fig. 2) and contralateral (Fig. 6) steady swimming emgs and during the time interval between left and right side swimming emgs. Because of the lack of a pattern between phase of the steady swimming emgs and the onset of the escape response, we conclude that the escape response can totally override the steady swimming motor pattern.

Figure 8 provides a schematic summary of muscle activity during steady swimming and both stages of the escape response. Details of the posterior propagation of steady swimming muscle activity in bluegills will be presented elsewhere. However, the narrow darkened areas in Fig. 8 do illustrate both the posterior propagation and the variable longitudinal extent of ipsilateral red muscle activity which periodically encompasses the entire length of the fish during steady swimming. Although the onset of stage 1 emgs is synchronous along the entire side of the fish, the slightly longer duration of the emg posteriorly can cause a brief time (2–3 ms) with only posterior stage 1 activity (not shown in Fig. 8). Because of the posterior propagation of the onset of stage 2, it takes an average of about 5 ms from the beginning of stage 2 until the entire side is simultaneously active. The average duration of about 17 ms for the stage 2 emg combined with the lags in the onset and offset time result in an interval of about 8 ms of stage 2 muscle activity along the entire side of the fish.

We could not always quantify the stage 2 emgs on all channels, but in all of our trials at least one channel always had a distinct burst of contralateral muscle activity that followed stage 1. Foreman and Eaton (1993) recently described escape responses with and without such a contralateral emg and with and without a resultant change in the escape trajectory angle (= angle 2 of Foreman and Eaton). Our kinematic analysis (combined with a preliminary analysis using the methods of Foreman and Eaton) indicated that all of our data were limited to just one of these two cases described by Foreman and Eaton (angle 2 present). Our particular experimental protocol was also probably responsible for decreasing the variability of our sample of escape emgs and trajectories compared to those described by Foreman and Eaton (1993) for which there was a contralateral emg.

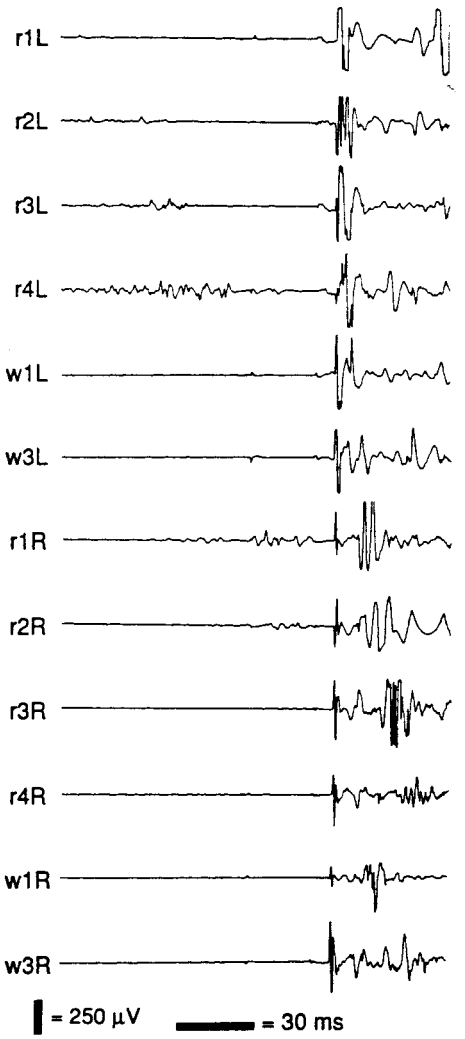

Fig. 6. Representative emgs from an escape response (concave left) that occurred during steady swimming muscle activity at the right anterior sites. These emgs are for the same individual as shown in Fig. 4

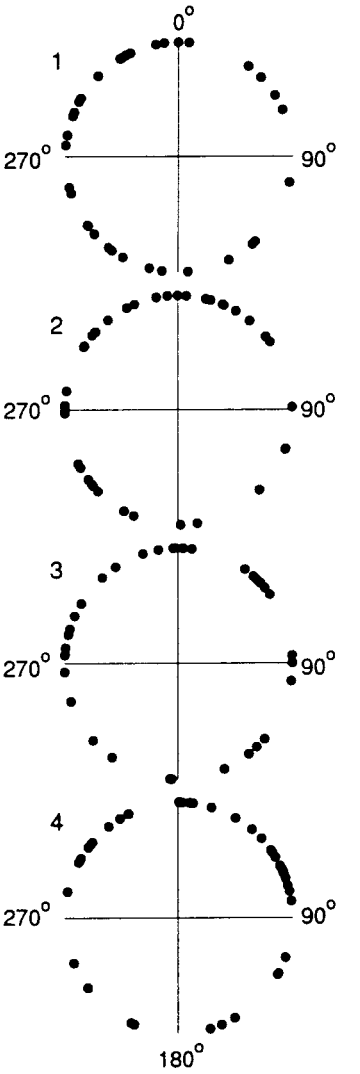

Fig. 7. Phase of the steady swimming muscle activity ipsilateral to the side of the stage 1 emg and at the time of stage 1 emg onset. The *number* to the upper left of each plot indicates the electrode position as illustrated in Fig. 1. Each *point* represents a single escape response, and its position in degrees around the circumference of the unit circle represents the phase of the steady swimming emg where 0° equals the onset of the steady swimming emg

Kinematics

Figure 9 shows representative reconstructed midlines at the beginning of the escape response and at the end of stage 1 and 2 emgs. Relative to the starting position, the skull and tail are displaced laterally towards the side of the stage 1 emg; however, the portion of the fish about from vertebrae 5 to 15 is displaced contralaterally. Figures 10 and 11 show lateral displacement (Y) and lateral flexion (A) versus time for the standard longitudinal locations along the length of a fish during a representative escape behavior. As a result of rapid, high amplitude lateral flexion between the head (approx. 20% of fish total length) and the first vertebra, the snout of the fish has a large lateral displacement during the stage 1 emg. In contrast, the first few vertebrae had appreciable lateral flexion but little detectable lateral displacement occurring during the stage 1 emgs. However, beginning near vertebra 5 (longitudinal location 3) there was a distinct maximal magnitude of contralateral displacement that was nearly coincident with the end of the stage 1 emgs, and

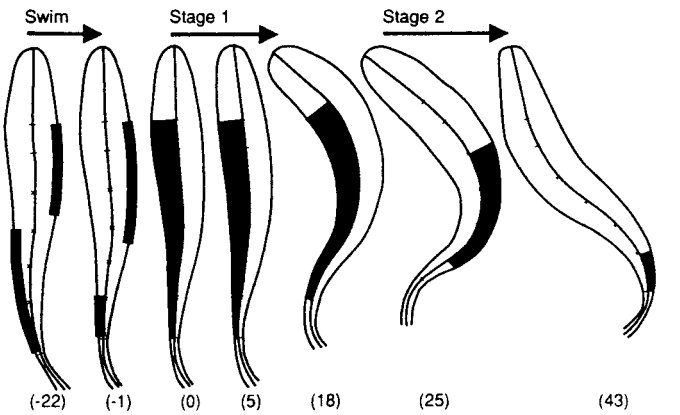

Fig. 8. Diagrammatic summary of muscle activity during swimming and both stages of the escape response based on the data in this paper. The muscle activity and outlines of the dorsal view of the fish are from a single individual. Times in ms are indicated parenthetically to the right of each figure (0 = onset of stage 1 emg). The *thin darkened lateral areas* represent a region of only red muscle activity, whereas the *thicker darkened areas* represent synchronous red and white muscle activity. *X marks* along the midline indicate the longitudinal location of electrode sites 1–4 (Fig. 1). From anterior to posterior, the 3 remaining marks on the midline indicate the posterior margin of the skull, vertebra 5, and the beginning of the caudal fin, respectively

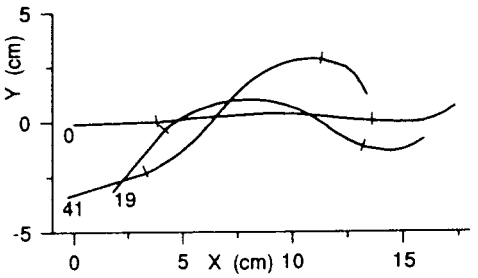

Fig. 9. Reconstructed midlines from one individual performing an escape response (trunk concave left stage 1). The midlines are shown with respect to our fixed frame of reference, and the marks on the midlines indicate the extent of the vertebral column (excluding tail bones). The snout of the fish is pointed to the left and the numbers indicate elapsed time in ms from the onset of the stage 1 emg. The midlines are at the beginning and end of the stage 1 emg and the end of the stage 2 emg

this kinematic landmark corresponding to the crest of a wave was also apparent for the remaining more posterior sites. Similarly, a maximum lateral flexion concave towards the side of the stage 1 emg occurred near the end of the stage 1 emg anteriorly, and this kinematic landmark could be detected at the additional more posterior sites.

Tables 3 and 4 summarize the results of the ANOVAs and means of the kinematic variables quantifying the timing of events as well as the lateral displacement and flexion during various intervals of the escape responses. All 12 of the kinematic variables varied significantly among the locations within the vertebral column that were used for the ANOVAs.

The times of maximal lateral displacement (TYMX), maximal lateral flexion (TAMX) and straightening of the vertebral column (TAMN) all increased from anterior to posterior. Therefore, the kinematic events involved in the escape response are propagated posteriorly despite the synchronous onset of the stage 1 emgs. Another unexpected finding was that the times of maximal lateral displacement and flexion (TAMX and TYMX) were not confined to a single stage of the escape response (as defined by the emg times). For example, maximal lateral displacement of the anterior, middle and posterior vertebral column often occurred at the end of stage 1 emg, end of stage 2 emg and about 10 ms after the end of stage 2 emg, respectively (Fig. 10, Table 4). The mean time of the end of the stage 2 emg was about 37 ms (Table 2 for site 4 add ON2 and DUR2) compared with a mean value of 46 ms for the time of maximal lateral displacement at the most posterior site within the vertebral column (7 in Table 4). The time of maximal lateral flexion (TAMX) showed a significant posterior increase along the length of the fish. Furthermore, posterior to the middle of the fish's body (excluding caudal vertebrae) maximal lateral flexion always preceded maximal lateral displacement (Table 4, TAMX & TYMX). Roughly at the time of maximal lateral flexion (TAMX = 35 ms) for the most posterior vertebrae, the middle vertebrae were straight (TAMN). None of the three kinematic timing variables varied significantly between the swimming and standstill trials (Table 3, TYMX, TAMX TAMN).

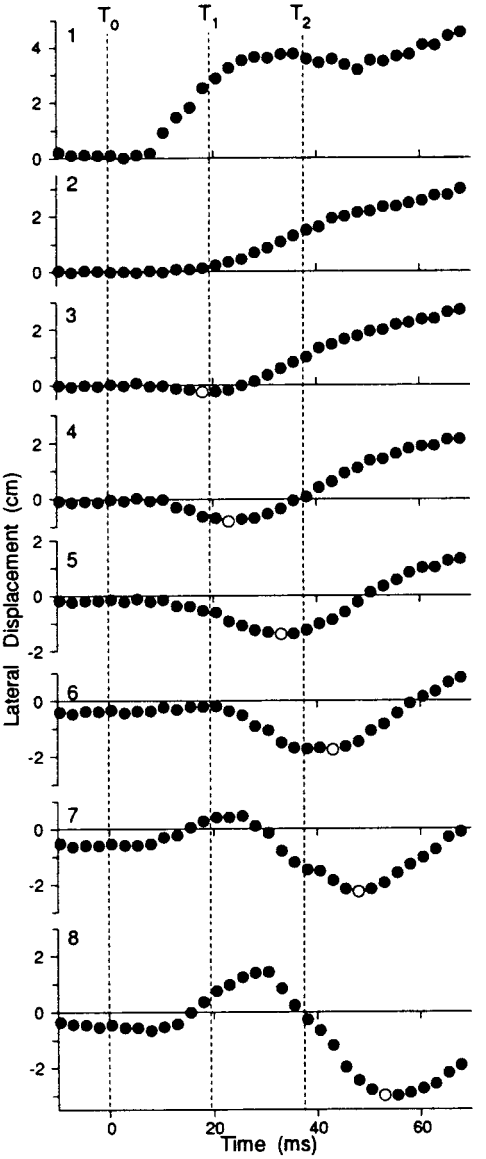

Fig. 10. Lateral displacement versus time for a single individual. T_0, T_1 and T_2 indicate the onset and latest offset of the stage 1 emg and the latest offset of the stage 2 emg, respectively. The *open symbols* indicate the points considered maximal lateral displacement. For each graph the *number at upper left* indicates the longitudinal position as indicated in Tables 3 and 4. Note that the scale of the y-axis is identical for all graphs

The highly significant longitudinal variation in the variables indicating lateral displacement during stages 1 and 2 (Y1, Y2) and from T_0 to TYMX (YMXR) is most easily understood by referring to Figs. 9 and 10. Negative mean values of Y1 for vertebrae 5–15 indicate that the displacement is contralateral to the side of the stage 1 emg, and then the direction of lateral displacement reverses during stage 2 ($Y2 > 0$). Interestingly, the posterior portion of the fish (Table 4, sites 6–7) is not displaced contralateral to the side of the stage 1 emg until sometime during the second stage of the escape response ($Y2 < 0$). For sites posterior to the skull, the amplitude of maximum lateral displacement (YMXR) increased nearly tenfold from anterior (3 mm) to posterior (30 mm). Although

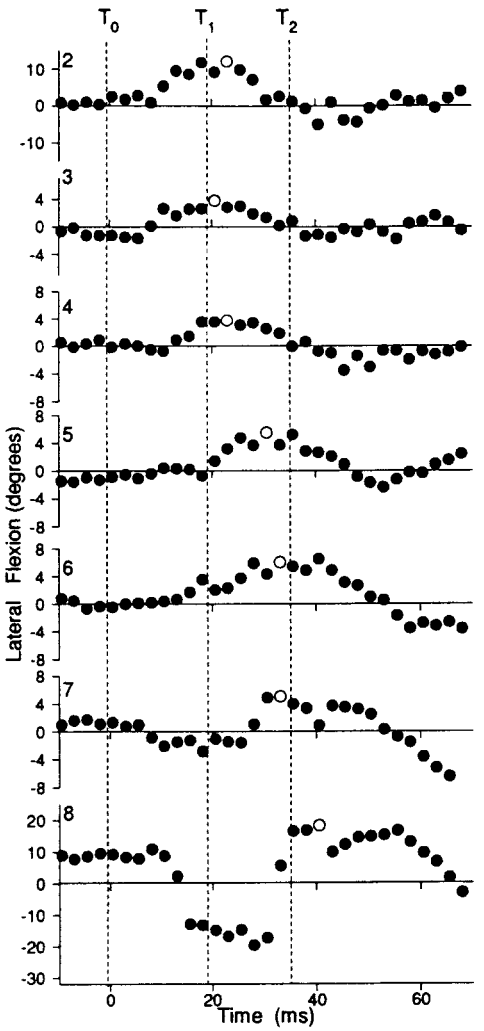

Fig. 11. Lateral flexion versus time for the same sequence as shown in Fig. 10. Abbreviations are as indicated for Fig. 10. Note that the scale of the y-axis is identical only for positions 3–7. *Open symbols* indicate the points considered maximal flexion.

the magnitude of the posterior increase in YMXR is striking, posterior increases in amplitude are commonplace for diverse types of undulatory swimming. Y2 and YMXR were the only two kinematic variables that clearly appeared to vary between swimming and standstill trials and their mean values are given separately for the two experimental conditions in Table 4. Figure 12 illustrates divergence in the mean values of the relative change in lateral displacement (YMXR) from anterior to posterior, with posterior means of YMXR from standstill trials being significantly greater than those for swimming. Consequently, there was also a highly significant interaction term between the site and swim factors in the ANOVA for YMXR. For the posterior sites, YMXR occurs during stage 2 or later, and the significant variation in Y2 between swimming and standstill trials is consistent with the observed differences in YMXR for the same comparison.

Of all of the kinematic variables quantifying lateral flexion, only the value of maximal lateral flexion (AMX) and the amount of flexion from T_0 to TAMX (AMXR) showed a tendency to differ between swimming and standstill trials (Table 3). The standstill trials tended to have slightly higher values of AMX and AMXR, and this is consistent with the statistically significant differences in Y2 and YMXR between swimming and standstill trials (Table 4). The nature of the statistically significant variation in lateral flexion at the ends of stages 1 and 2 (AT1 and AT2) revealed the unexpected result that, at the ends of both stages, the body of the fish is not entirely concave towards the side of the immediately preceding emg. Although the sites along the trunk of the fish are concave towards the side of the stage 1 emg (Table 4), near vertebra 20 the vertebrae are nearly straight, and more posteriorly the vertebrae are convex towards the side of the stage 1 emg. This pattern of lateral flexion opposite to the side of the emg is even more pronounced at the end of stage 2 where the posterior vertebrae flexed 4–5 degrees convex to the side of the stage 2 emg, and these same sites had maximal observed values of lateral flexion of only about 6.5 degrees. Finally, we quantified the amount of

Table 3. Summary of F-tests from 3-way ANOVAs performed separately on each of the 12 kinematic variables. Factors and labeling conventions are as in Table 1. See Materials and methods for more details of experimental design, variable abbreviations, and sample sizes

Kinematic Variable	Three-way ANOVA Effects						
	Site (A) 4–5	Swim (B) 1	Fish (C) 3	A*C 12–15	B*C 3	A*B 4–5	A*B*C 12–15
TYMX (195)	960.6**	5.2	10.5**	0.8	12.5**	3.8*	0.3
TAMX (234)	341.4**	3.2	9.7**	0.5	4.9**	1.3	0.3
TAMN (226)	381.9**	0.7	11.0**	0.7	8.3**	2.7′	0.2
Y1 (234)	216.0**	0.8	0.3	2.2*	1.0	1.8	1.8*
Y2 (234)	318.0**	10.5*	1.5	1.6′	2.1′	0.8	2.3*
YMXR (195)	351.5**	62.0*	10.0**	0.6	1.0	210.4**	0.0
A1 (195)	97.7**	1.3	1.3	1.0	1.7	1.7	1.4
A2 (195)	183.3**	0.6	2.3′	1.6′	6.2*	0.8	1.0
AMXR (195)	11.3**	6.6′	4.0*	3.1*	1.7	0.8	0.7
AMX (195)	14.2**	7.3′	1.2	3.2**	1.4	1.6	1.1
AT1 (195)	243.9**	2.1	3.2*	0.5	3.2*	1.4	1.8*
AT2 (195)	105.0**	0.0	2.2′	1.6′	3.6*	3.6*	0.5

Table 4. Means (SD) of kinematic variables. All times, displacements and angles are in ms, mm, and degrees, respectively. *sw* = swimming trials only ($n = 31$); *st* = standstill trials only ($n = 16$), and *all* = pooled data from sw + st

Kinematic Variable		Longitudinal Site							
		1	2	3	4	5	6	7	8
TYMX	all			16.5 (2.7)	22.2 (3.4)	30.2 (3.5)	37.8 (3.7)	45.7 (3.4)	52.4 (3.7)
TAMX	all		16.0 (2.9)	18.2 (3.3)	21.4 (3.6)	26.2 (3.9)	29.8 (4.2)	34.9 (4.4)	42.0 (4.5)
TAMN	all		27.7 (4.5)	30.9 (4.3)	35.6 (3.7)	43.5 (4.2)	49.1 (4.3)	54.6 (4.8)	61.1 (5.6)
Y1	all	20.3 (5.7)	1.5 (1.2)	2.3 (0.8)	−5.2 (1.5)	−3.6 (1.5)	0.8 (0.7)	6.3 (1.8)	9.2 (3.4)
Y2	st	10.3 (9.0)	14.5 (3.2)	12.4 (3.8)	5.1 (5.6)	−8.7 (4.6)	−19.6 (4.3)	−23.6 (7.6)	−14.8 (13.3)
Y2	sw	6.8 (10.5)	14.6 (5.1)	13.4 (4.5)	7.3 (4.2)	−4.9 (3.8)	−14.9 (3.4)	−19.3 (6.8)	−11.7 (11.6)
YMXR	st			−3.1 (1.7)	−9.9 (3.1)	−16.7 (4.4)	−23.1 (6.1)	−30.4 (7.4)	−38.2 (7.6)
YMXR	sw			−2.8 (1.1)	−8.1 (2.3)	−13.1 (3.1)	−16.7 (4.2)	−21.5 (5.4)	−27.3 (7.7)
A1	all		8.7 (3.4)	2.3 (1.4)	3.1 (1.2)	1.3 (1.2)	0.9 (0.9)	−1.2 (0.9)	−10.7 (5.5)
A2	all		−13.6 (4.1)	−3.9 (1.9)	−3.1 (1.9)	1.0 (2.1)	3.6 (1.4)	6.5 (1.6)	23.8 (8.1)
AMXR	st		9.9 (2.9)	3.9 (1.0)	4.9 (1.1)	5.0 (1.0)	6.6 (1.6)	6.7 (1.6)	19.8 (5.9)
AMXR	sw		9.7 (3.3)	3.5 (1.5)	4.5 (1.2)	4.7 (1.0)	5.6 (1.1)	6.0 (1.7)	18.5 (6.0)
AMX	st		10.2 (2.9)	3.6 (0.9)	4.5 (1.0)	5.3 (1.1)	6.2 (1.1)	6.4 (1.1)	18.4 (4.5)
AMX	sw		9.5 (2.3)	3.5 (1.3)	4.4 (0.8)	5 (0.9)	5.4 (0.8)	5.5 (1.3)	17 (3.7)
AT1	all		8.6 (2.9)	2.3 (1.2)	2.9 (1.0)	1.6 (1.1)	0.7 (1.1)	−1.6 (0.9)	−12.2 (4.5)
AT2	all		−5.0 (3.1)	−1.6 (1.5)	−0.2 (1.7)	2.5 (1.9)	4.2 (1.2)	4.9 (1.3)	11.6 (7.3)

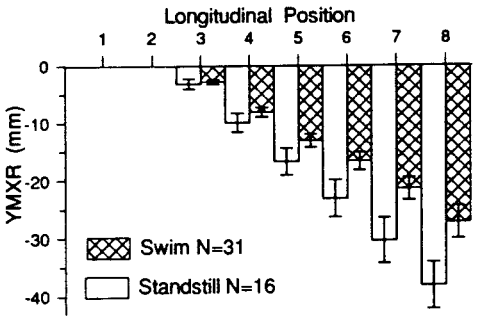

Fig. 12. Mean maximum lateral displacement relative to initial position (YMXR) with 95% CL pooled for all observations of fish swimming or at a standstill. See Table 1 for tests of significance

vertebral flexion that occurred during stages 1 and 2 (A1 and A2) to clarify the combination of initial conditions and movement responsible for the posture at single points in time. The significant longitudinal variation in A1 and A2 (Table 3) showed a pattern of flexion towards the side of the emg anteriorly and bending towards the opposite side posteriorly. The magnitudes of the flexing movements during stage 2 were generally greater than those of stage 1 (Table 4).

Discussion

The following major conclusions can be drawn from our analysis of muscle activity and midline kinematics for the escape response. 1) Red and white muscle were usually simultaneously recruited during both stages of the escape behavior. 2) Much of the electrical activity of the posterior axial musculature correlated with a pattern of lateral bending that suggests lengthening of the contractile tissue. 3) The duration of the stage 1 emgs increased posteriorly along the length of the fish. 4) Stage 2 muscle activity was propagated posteriorly. 5) All kinematic events were propagated posteriorly rather than forming a "standing" wave. 6) Escape responses can occur at any phase with respect to the steady swimming motor pattern. 7) Only two of twelve kinematic variables (YMXR, Y2) varied significantly between escape responses elicited from swimming fish versus those at a standstill.

Because of the spatial segregation of the different fiber types of the axial muscles of fish, they have been a useful model for understanding general patterns of fiber type recruitment. In fact, most early electromyographic studies of the undulatory swimming of fishes concentrated almost entirely on this issue of fiber type recruitment while giving minimal attention (if any) to the accompanying kinematics (Bone 1966; Rayner and Keenan 1967; Hudson 1973). Additional studies have found that the effects of decreasing body temperature of swimming fish parallel those of increased swimming speed which initially causes increased intensity of the recruitment of red muscle up to some threshold speed whereupon a faster fiber type, such as white muscle, is recruited (Rome et al. 1984, 1992a). Hence, the fiber type recruitment during the escape response resembles that for high speed swimming in that faster fiber types are not recruited exclusively; instead they are recruited in addition to the slower fiber types.

Because of the extreme rapidity of escape response of fishes, this behavior has figured prominently in attempts to understand the limits of muscular performance of fishes. For example, Rome and Sosnicki (1991) documented the sarcomeric lengths of red and white muscle in carp that were fixed in a position similar to that of an escape response. When combined with the observed relationship between sarcomeric length and force generating capacity for frog muscle, Rome and Sosnicki (1991) suggested that the carp red and white muscle would be operating at 50% and 96% of their maximum force generating capacity, respectively; hence, they considered the use of red

muscle unlikely during they escape response. The neuroanatomy of the relatively small secondary motoneurons innervating the red muscle of fish has also been used to support the prediction of no activity of the red muscle during the escape behavior (Fetcho 1991). Rome et al. (1992b) have suggested that a general feature of muscle activity is that it occurs over a limited range of V/Vmax (shortening velocity divided by maximal shortening velocity) where the muscle tissue is most effective mechanically. However, our findings of red muscle activity during both stages of the escape combined with posterior activity during lengthening contradict these plausible predictions that were based on muscle physiology, neuroanatomy, and mechanics.

Several studies of steady undulatory swimming have found muscle activity during lengthening in the posterior regions of such diverse animals as eels, trout, carp, and even snakes (Grillner and Kashin 1976; Williams et al. 1989; Van Leeuwen et al. 1990; Jayne 1988). In contrast to the rather complicated patterns of activity observed during steady swimming, it seemed quite plausible that stage 1 muscle activity would conform to simple activity during shortening because of the lack of either prior motion or antagonistic muscle activity. However, mean values at the end of both stages of muscle activity indicate that most of the posterior muscle activity is resisting bending rather than actively causing flexion towards the side of muscle activity.

Our values of lateral vertebral flexion (A) can be converted to estimates of the % resting muscle length assuming that the superficial, longitudinally oriented fibers, located at the widest part of the fish keep pace with the changing curvature of the fish. The estimate is based on adding 100% to the ratio of the lateral to midline radii of curvature which equals 100*((L/(2*sin A/2))–W/2)/(L/(2*sin A/2)), where L is the average vertebral length of the pair of vertebrae, W is the width of the body at a particular intervertebral joint. Using the data from the four bluegill for which we analyzed both the emgs and kinematics, mean body widths from anterior to posterior at the four locations of the red electrodes were 22.5, 18.0, 12.5 and 9.0 mm, respectively, and mean values of L at these same sites were 4.3, 4.1, 3.6 and 3.3 mm, respectively. Substituting mean values of bending at the end of the stage 1 emgs (2.9°, 1.6°, 0.7° and −1.6°) yields relative muscle lengths of 87, 94, 98 and 104%, respectively on the side of the stage 1 emg. Similarly, for the mean lateral flexion at the end of stage 2 (0.2°, −2.5°, −4.2°, and −4.9°) estimates of relative muscle lengths on the side of the stage 2 emg were 99, 110, 113 and 112% of resting length, respectively. Allowing for the starting position of the fish at the end of stage 1, during stage 2 muscle on the side of the stage 2 emg near the electrode sites undergoes total length changes of −14, 4, 11 and 16% of resting length, respectively. Dividing by the mean duration of stage 2 (18 ms) conservatively estimates the shortening speeds (7.8, −2.2, −6.1 and −8.9 muscle lengths/s, respectively) required to keep pace with the changing curvature (negative values indicate muscle lengthening). Although the more medial position and oblique orientation of the white myomeric musculature causes less muscle strain (Rome and Sosnicki 1991) than was calculated above, these estimates of superficial muscle strain and strain rates emphasize the striking longitudinal differences in the manner in which muscle is utilized during the escape behavior.

Blight's (1977) insightful review of vertebrate aquatic undulatory locomotion emphasized that the observed patterns of bending in an undulating swimmer depend on the complicated interactions of the passive mechanical properties of the body of the swimmer, the pattern of force production intrinsic to the swimming body, and the effects of the resistance of the fluid acting on the body of the swimmer. Blight (1977) hypothesized that if an undulating rod was "dominated" by the resistive forces of the water, then it would flex such that a concavity would be formed in the opposite direction of the movement of the rod through the water. Our observations on the posterior lateral flexion of the vertebral column and the extensive muscle activity during lengthening conform closely to the expectation for such a resistance dominated rod. Rather than performing positive work, much of the posterior muscle activity during the escape response appears to counteract the resistive forces imposed by the fluid.

Blight (1976) also proposed that given appropriate passive mechanical properties, an undulating body could propagate mechanical waves of bending even though the pattern of muscle activity might resemble a standing wave rather than a posteriorly propagated wave. This conclusion of Blight was based on emgs recorded from small newts. However, because Blight did not quantify the emgs, and he only recorded from two longitudinal positions, the experimental support for this conclusion seems questionable. Furthermore a recent electromyographic study of salamanders (Frolich and Biewener 1992) found the general vertebrate pattern of swimming muscle activity which is posterior propagation. Of all the undulatory vertebrate locomotor behaviors that have been described, stage 1 of the escape response appears to have muscle activity most closely resembling that of a standing wave (Figs. 4 and 6).

However, despite the standing wave pattern of stage 1 onset of muscle activity, our quantitative analysis revealed that the offset times of the stage 1 emg had significant posterior propagation resulting in longer durations of posterior emgs (Tables 1 and 2). The mean duration of the most posterior site (14.7 ms) was approximately 28% longer than that of the most anterior site. This longitudinal variation in stage 1 emg duration lag times is the reverse of that observed for the steady swimming of bluegill in our experiments where the mean relative emg duration at electrode location 1 was approximately 38% longer than that observed at electrode location 4. Such a posterior decrease in emg duration appears to be a general feature of the steady swimming of other species of fish with a generalized body shape (Williams et al. 1989; Van Leeuwen et al. 1990). Interestingly, the stage 2 emg duration showed no significant variation among the different longitudinal locations. Thus, we have observed all possible combinations of change in emg duration including: 1) a posterior decrease (steady swimming), 2) a posterior

Table 5. Lag times (ms) between mean emg and kinematic events at homologous longitudinal sites. *OFF1* (=DUR1) and *OFF2* (=ON2+DUR2) are the offset times of the stage 1 and 2 emgs, respectively, and other variables are as in Tables 1–4

Variable Pair	Longitudinal Site				
	3	4	5	6	7
TAMX-OFF1		9.9	12.8	16.3	20.2
TAMX-ON2		7.2	9.1	10.2	16.5
TAMX-OFF2		−10.2	−8.5	−5.4	−1.7
TYMX-TAMX	−1.7	0.8	4.0	8.0	10.8
TYMN-TAMX	12.7	14.2	17.3	19.3	19.7
TYMX-OFF2		−9.4	−4.5	2.6	9.1
TAMN-OFF2		4.0	8.8	13.9	18.0
TAMN-TYMX	14.4	13.4	13.3	11.3	8.9

increase (stage 1), and 3) no change along the length of the bluegill (stage 2).

A striking feature of the kinematics of the escape response of the bluegill was the posterior propagation of both lateral bending and maximum lateral displacement. Furthermore, these two kinematic variables showed no obvious discontinuity when viewed across the time intervals of the stage 1 and stage 2 emgs. It is not immediately obvious how important the posterior increase in the duration of the stage 1 emg is for initiating the posterior propagation of kinematic events. Some insight into this issue can be gained by looking at the kinematic variables along the entire length of the fish at the moment of the earliest offset of a stage 1 emg. For the sequence illustrated in Figs. 10 and 11, the offset of the most anterior stage 1 emg was 11 ms after the onset of stage 1 and 8 ms (3 symbols in plot = 7.5 ms) before the latest offset which was used to delineate T1. Close examination of Fig. 11 reveals that maximal lateral bending had not yet occurred for any longititudinal location by the earliest stage 1 offset time. However, for longitudinal sites 2 and 3 the first conspicuous lateral flexion begins approximately 7.5 ms after the stage 1 onset whereas at longitudinal site 4 the first noticeable lateral flexion occurs about 2.5 ms later. Similar close scrutiny of the other plots of lateral flexion versus time often revealed that a lag in the time of initial lateral flexion was present while the entire side of the fish still had simultaneous stage 1 muscle activity. Therefore, the posterior propagation of kinematic events during stage 1 can not be attributed entirely to the posterior increase in emg duration. It remains an open question whether or not the posterior increase in stage 1 emg duration enhances the initial posterior propagation of kinematic events. The underlying neural basis for the longitudinal differences in the stage 1 emg offset would also be a fruitful area for future study.

Although all kinematic and emg events after the onset of stage 1 were propagated posteriorly, longitudinal variation in the lag time between pairs of variables indicates that the rates of propagation differ among the various quantities (Table 5). For example, at the third longitudinal site, the negative lag time (–1.7 ms) between the time of maximal lateral displacement and that of maximal lateral flexion (TYMX-TAMX) indicates that the former event (TYMX) preceded the latter event (TAMX) of the pair, but there is a progressive posterior increase in the lag times between the variables at each site until, at site 7, TYMX follows TAMX by more than 10 ms. Therefore, maximal lateral displacement (TYMX) is propagated posteriorly more slowly than maximal lateral bending (TAMX). Additional comparisons of the longitudinal variation in the lag times between kinematic and emg events indicate that emg events were always propagated posteriorly faster than kinematic events (Table 5). Similarly, several studies of the steady undulatory swimming of a wide variety of vertebrates (eels: Grillner and Kashin 1976; trout: Williams et al. 1989; salamanders: Frolich and Biewener 1992; snakes: Jayne 1988) have also found that the rate of propagation of muscle activity exceeds that of the kinematic events. Close examination of Table 5 indicates that virtually no pair of kinematic variables or combinations of kinematic and emg variables had a constant lag time along the entire length of the fish. Consequently, the phase relationships among all variables change with the longitudinal position within the fish. The fact that lateral displacement and maximal lateral flexion were out of phase was a particularly unexpected finding, since these two variables are often assumed to be in phase for undulatory locomotion.

Our analysis of the escape responses that were elicited during the steady swimming of bluegills (Fig. 7) indicates that the escape behavior can occur at any time with respect to the phase of the steady swimming motor pattern. Recent extracellular recordings of the nerves in fictive swimming preparations of goldfish (Fetcho 1992) and amphibian larvae (Lee and Olin 1992) have found that stimulating the Mauthner cell during the steady swimming motor pattern always produces an output of the motor axons (in the dorsal ramus of the ventral root) characteristic of the muscle activity involved in the escape response, regardless of the phase of the steady swimming motor pattern. In these fictive preparations, the rhythmic motor pattern of steady swimming was disrupted by the escape behavior motor pattern, but after a short time lag, the rhythmic steady swimming motor pattern resumed. An interesting unanswered question for intact swimming fish is whether or not the escape behavior could override a motor pattern of high speed swimming that included white muscle activity. As shown in Fig. 5, while bluegills were swimming steadily at speeds less than two lengths per second, they recruited exclusively red muscle. When we attempted to elicit swimming sufficiently fast to involve the white axial muscle, the bluegills routinely switched to a burst and glide mode of swimming. Because of the non-periodic nature of this swimming mode as well as the unpredictable timing of the bursts of swimming, it was not practical to elicit the escape behavior during this type of swimming. In fishes the cell bodies of red motor neurons are smaller and somewhat spatially segregated from the motor neurons of the white musculature (Fetcho 1986). Furthermore, the correlation between the taxonomy of fishes and different patterns of innervation of the white muscle lead Bone (1978) to suggest that one group of fishes (including goldfish) was more likely to use the white musculature during

steady swimming, whereas other groups of fishes (including the bluegill) were more likely to use the white muscle exclusively for burst swimming. Thus, it is still of interest to determine the generality of this finding that the Mauthner initiated escape response can totally override the steady swimming motor pattern by examining other fish taxa.

Despite the ability to perform an escape response during steady swimming, some subtle differences did exist between those escape responses performed at a standstill and those during swimming (Table 3). Escape responses during swimming had decreased mean values of the amount of maximum lateral displacement (YMXR, Y2) occurring mainly during stage 2 and later in the posterior portion of the fish (Fig. 12). Interestingly, when these two kinematic variables were plotted versus the phase of the steady swimming motor pattern at the onset of the escape, no clear pattern of variation was present. Instead of a particular phase of the steady swimming motor pattern (such as steady swimming muscle activity contralateral to the stage 1 emg) adversely affecting the amplitude of maximum lateral displacement, it appears that any steady swimming muscle activity prior to an escape response will have a slight adverse effect on the performance of the escape response. In a centrarchid species closely related to the bluegill sunfish, the bass *Micropterus*, Johnson et al. (unpublished) found that the mean time to peak tension for a twitch in the red muscle is 45 ms and the time to one-half relaxation is greater than 70 ms, whereas for white muscle these times are 11 and 18 ms, respectively at 20°C. Given that the mean time from the onset of stage 1 to the offset of the stage 2 emg is only 36.6 ms (Table 2), it seems likely that a significant fraction of the red muscle force will always be opposing some of the movements during either stage 1 and stage 2 regardless of the side and longitudinal location of the steady swimming emgs immediately prior to the escape response. These data on the time course of force development and relaxation also suggest the minimal utility in activating the red muscle during stage 1.

Because the amount the red muscle in centrarchids may be less than 2% of the total fish mass (Johnson et al., unpublished), one would expect that the force produced by recruiting all of the white muscle could trivialize the effect of prior red muscle activity. Indeed, for the bluegill, only the amplitude of two kinematic variables was affected, whereas the time course of the kinematic events in the escape response did not differ among swimming versus standstill trials. The tremendous differences in the abilities of different fishes to sustain high speed swimming is correlated in part to the relative amount of red muscle. Hence, it would be intriguing to determine the tradeoffs in performance that may exist with fast starts, especially in light of the fact that activation of red muscle during stage 1 should cause residual force opposing the stage 2 muscle activity.

Acknowledgements. We thank J. Fetcho for many lengthy discussions which largely motivated this study. R. Eaton and M. Foreman graciously provided a prepublication copy of their manuscript, and R. Eaton freely offered useful insights. We are grateful to J. Seigel and the Section of Fishes at the Los Angeles County Museum for the x-rays of specimens. H. Nguyen, A. Lozado and B. Malas laboriously digitized many video images. Support was provided by NSF grants BNS 8919497 to BCJ and GVL and NSF BSR 9007994 to GVL. The high-speed video system was obtained under NSF BBS 8820664.

References

Blight AR (1976) Undulatory swimming with and without waves of contraction. Nature 264:352–354

Blight AR (1977) The muscular control of vertebrate swimming movements. Biol Rev 52:181–218

Bone Q (1966) On the function of the two types of myotomal muscle fiber in elasmobranch fish. J Mar Biol Assoc UK 46:321–349

Bone Q (1978) Locomotor muscle. In: Hoar WS, Randall DJ (eds) Fish physiology. Vol 7. Locomotion. Academic Press, New York, pp 361–424

Covell JW, Smith M, Harper DG, Blake RW (1991) Skeletal muscle deformation in the lateral muscle of the intact rainbow trout *Oncorhynchus mykiss* during fast start maneuvers. J Exp Biol 156:453–466

Eaton RC, Emberley DS (1991) How stimulus direction determines the trajectory of the Mauthner-initiated escape response in a teleost fish. J Exp Biol 161:469–487

Eaton RC, Hackett JT (1984) The role of the Mauthner cell in fast-starts involving escape in teleost fishes. In: Eaton RC (ed) Neural mechanisms of startle behavior. Plenum Press, New York, pp 213–266

Eaton RC, Bombardieri RA, Meyer DL (1977) The Mauthner-initiated startle response in teleost fish. J Exp Biol 66:65–81

Eaton RC, Lavender WA, Wieland CM (1981) Identification of Mauthner-initiated response patterns in goldfish: evidence from simultaneous cinematography and electrophysiology. J Comp Physiol 144:521–531

Eaton RC, Lavender WA, Wieland CM (1982) Alternative neural pathways initiate fast-start responses following lesions of the Mauthner neuron in goldfish. J Comp Physiol 145:485–496

Eaton RC, DiDomenico R, Nissanov J (1988) Flexible body dynamics of the goldfish C-start: implications for reticulospinal command mechanisms. J Neurosci 8:2758–2768

Eaton RC, DiDomenico R, Nissanov J (1991) The role of the Mauthner cell in sensorimotor integration by the brainstem escape network. Brain Behav Evol 37:272–285

Fetcho JR (1986) The organization of the motoneurons innervating the axial musculature of vertebrates. I. Goldfish (*Carassius auratus*) and mudpuppies (*Necturus maculosus*). J Comp Neurol 249:521–550

Fetcho JR (1991) Spinal network of the Mauthner cell. Brain Behav Evol 37:298–316

Fetcho JR (1992) A single action potential in a reticulospinal neuron can reset the fictive swimming rhythm in goldfish. Soc Neurosci Abstr No. 140.1

Foreman MB, Eaton RC (1993) The direction change concept for reticulospinal control of goldfish escape. J Neurosci 13:4101–4113

Frolich LM, Biewener AA (1992) Kinematic and electromyographic analysis of the functional role of the body axis during terrestrial and aquatic locomotion in the salamander *Ambystoma tigrinum*. J Exp Biol 162:107–130

Gray J (1968) Animal locomotion. Weidenfield and Nicolson, London

Grillner S, Kashin S (1976) On the generation and performance of swimming in fish. In: Herman R, Grillner S, Stein, Stuart D (eds) Neural control of locomotion. Plenum Press, New York, pp 181–202

Harper DG, Blake RW (1990) Fast-start performance of rainbow trout *Salmo gairdneri* and Northern pike *Esox lucius*. J Exp Biol 150:321–342

Hudson RCL (1973) On the function of the white muscles in teleosts at intermediate speeds. J Exp Biol 58:509–522

Jayne BC (1988) Muscular mechanisms of snake locomotion: An electromyographic study of the lateral undulation of the Florida banded water snake (*Nerodia fasciata*) and the yellow rat snake (*Elaphe obsoleta*). J Morphol 197:159–181

Johnston IA (1991) Muscle action during locomotion: a comparative perspective. J Exp Biol 160:167–185

Lee MT, Olin AM (1992) Interaction between Mauthner neurons and the swimming pattern generator in *Xenopus* tadpoles. Soc Neurosci Abstr No. 139.16

Rayner MD Keenan MJ (1967) Role of red and white muscles in the swimming of the skipjack tuna. Nature 214:392–393

Rome LC, Sosnicki AA (1991) Myofilament overlap in swimming carp II. Sarcomere length changes during swimming. Am J Physiol 260 (Cell Physiol 29): C289–C296

Rome LC, Loughna, PT, Goldspink G (1984) Muscle fiber recruitment as a function of swim speed and muscle temperature in carp. Am J Physiol 247: R272–R279

Rome LC, Choi IH, Lutz G, Sosnicki A (1992a) The influence of temperature on muscle function in the fast swimming scup I. Shortening velocity and muscle recruitment during swimming. J Exp Biol 163:259–279

Rome LC, Sosnicki A, Choi IH (1992b) The influence of temperature on muscle function in the fast swimming scup II. The mechanics of red muscle. J Exp Biol 162:281–295

Van Leeuwen JL, Lankheet MJM, Akster HA, Osse JWM (1990) Function of red axial muscles of carp (*Cyprinus carpio*): recruitment and normalized power output during swimming in different modes. J Zool Lond 220:123–145

Wardle CS (1975) Limit of fish swimming speed. Nature 255:725–727

Webb PW (1975) Hydrodynamics and energetics of fish propulsion. Bull Fish Res Board Can 190

Webb PW (1978) Fast start performance and body form in seven species of teleost fish. J Exp Biol 74:211–226

Webb PW, Skadsen JM (1980) Strike tactics of *Esox*. Can J Zool 58:1462–1469

Weihs D (1973) The mechanism of rapid starting of slender fish. Biorheology 10:343–350

Williams TL, Grillner S, Smoljaninov VV, Wallen P, Kashin S, Rossignol S (1989) Locomotion in lamprey and trout: the relative timing of activation and movement. J Exp Biol 143:559–566

Zar JH (1984) Biostatistical analysis. Prentice Hall, Englewood Cliffs, New Jersey

Zottoli SJ (1977) Correlation of the startle reflex and Mauthner cell auditory responses in unrestrained goldfish. J Exp Biol 66:243–254